3.3 New Processes for Alcohols and Oxygenated Fuel Additives

3.3.1 Oxygenate via Synthesis Gas

3.3.1.1 Overall 1QFY95 Objectives

(i) Complete the kinetic analysis of the methanol/isobutanol and ethanol/isobutanol coupling reactions to form ethers and dehydration reactions to form olefins and dimethylether over Amberlyst-35.

(ii) Conclude the experimental research and computational modelling of selective dimethylether synthesis from methanol/isobutanol mixtures over H-mordenite.

(iii) Complete all experiments using isotopically labelled ethanol and chiral alcohols over Nafion-H and Amberlyst-35 catalysts and write a detailed report that clarifies the mechanistic pathways that control product composition in the synthesis of ethers from alcohols.

(iv) Make substantial progress in establishing the accessibility, number, type (Lewis or Bronsted) and strength of the active surface acid sites by volumetric and HR-XPS analyses after pyridine adsorption on the sulfated zirconia catalyst that is highly active for the selective dehydration of isobutanol to isobutene from methanol/isobutanol reactant mixtures.

(v) Continue studies of increasing the surface area and catalytic activity of $Cs/Cu/ZnO/Cr_2O_3$ catalysts for higher alcohol synthesis from H_2/CO synthesis gas and review methods to attain high surface area Cu/ZrO_2 catalysts that are candidates for the synthesis of C_1-C_5 alcohols, in particular, branched products such as isobutanol.

3.3.1.2 Results and Discussion

A. Kinetic Analysis of Methanol/Isobutanol and Ethanol/Isobutanol Coupling Reactions

A systematic study of the dehydration and coupling of alcohols, i.e., methanol/isobutanol and ethanol/isobutanol binary mixtures, was previously carried out over the Amberlyst-35 resin catalyst, and kinetic analysis of the large amount of acquired experimental data was continued. A 2-page abstract entitled "Kinetic Evaluation of the Direct Synthesis of Ethers From Alcohols Over Sulfonated Resin Catalysts" was submitted for a presentation [1] at the First World Conference on Environmental Catalysis that will be held in Pisa, Italy during May 1-5, 1995. A draft of the 4-page manuscript that will be included in the proceedings volume has been written and is being revised. An expanded 8-page manuscript is being prepared for publication in a special issue of Catalysis Today.

B. Selective DME Synthesis Over H-Mordenite

Final experiments were carried out and reported during the previous quarter. A comprehensive report on this research will be written.

C. Mechanistic Pathways for Ether Synthesis

No additional experiments were carried out, but computations centered on the S_N2 reaction of ethanol with chiral S-2-pentanol were completed. The goal was to determine if the transition state complex formed by the coupling reaction would be accommodated in the H-ZSM-5 zeolite.

The geometry of the transition state was optimized by using the Spartan *ab initio* program (RHF/STO-3G model). It was found that the transition state could be accommodated at the intersection of the channel structure of the zeolite. The results indicate that the acid sites at the intersection of the two types of channels are responsible for catalyzing the dehydrative coupling of ethanol and 2-pentanol to the chiral 2-ethoxypentane product with very high selectivity to the inversion product. A communication has been written for publication, and it is near a final version that incorporates a graphic representation of the transition state complex.

In addition, previously obtained experimental data, reported in part in quarterly technical progress reports for January-March 1994 [2] and April-June 1994 [3] (Alternative Fuels I program), have been analyzed in greater detail and included in a communication [4] to be presented at a symposium sponsored by the Division of Fuel Chemistry at the national meeting of the American Chemical Society in Anaheim, CA in May 1995. The manuscript is entitled "Mechanistic Studies of the Pathways Leading to Ethers *via* Coupling of Alcohols," co-authored by Q. Sun, L. Lietti, R. G. Herman, and K. Klier. In particular, the reaction mechanisms for the solid acid-catalyzed dehydrative coupling of methanol and ethanol with isobutanol and 2-pentanol to form ethers were examined by using the data from the previous isotopic labelling, i.e., 180-ethanol, and chiral inversion experiments. It was shown that the solid acid-catalyzed direct coupling of alcohols to form ethers over Nafion-H, Amberlyst-35, and H-ZSM-5 zeolite proceeds primarily through a surface-mediated S_N2 reaction pathway that is far more efficient than either a carbenium or olefin pathway. However, the methyl tertiarybutyl ether (MTBE) and ethyl tertiarybutyl ether (ETBE) products were formed *via* a carbenium intermediate. The efficient surface S_N2 reaction gave rise to high selectivity to configurationally inverted chiral ethers when chiral alcohols were used. This was especially observed in the case of the H-ZSM-5 zeolite catalyst with ethanol/2-pentanol reactants, in which the minor carbenium ion or olefinic intermediate paths were further suppressed by "bottling" of the 3-ethoxypentane product by the narrow zeolite channels and 97% inversion of the chiral center was observed.

D. Investigation of Surface Acidity by X-Ray Photoelectron Spectroscopy

The surface acidity of solid superacids can be determined by measuring core level binding energy shifts obtained by X-ray photoelectron spectroscopy (XPS). The binding energy measured is related to the charge on the atom being investigated, i.e., an increase in the positive charge on an atom yields an increase in the measured binding energy. For solid acids, it is expedient to adsorb nitrogen-containing bases such as pyridine or ammonia because the nitrogen 1s core level is very sensitive to changes in the environment, e.g., charge on the atom. The N 1s binding energy for pyridine increased by 2-3 eV upon protonation to form the pyridinium ion. This occurred when pyridine was adsorbed on and interacted with Brönsted-type solid acids. The resultant N 1s binding energy shift was readily measured by XPS. Our research using this technique has shown that the sulfated zirconia catalyst has accessible both Lewis and Brönsted acid sites, with the Lewis acid sites having lower N 1s binding energy of adsorbed pyridine than the Brönsted sites. A few additional XPS analyses have been carried out during this quarter, and they will be described in a full report that is currently being written.

A number of computational methods have been employed to calculate the charge on the nitrogen atom in pyridine and pyridinium ion to aid in the quantitative measurement of acidity. The charges have been calculated using electronegativities and partial ionic character [5] and by

partial equalization of orbital electronegativity [6]. The computational results are being compared with experimental XPS results, and further refinements are being incorporated into the calculations being carried out.

E. Alcohol Synthesis Catalysts

During the previous quarter, a $Cu/ZnO/Cr_2O_3$ catalyst was prepared *via* coprecipitation of a hydrotalcite-like percursor using a standard procedure [7], and it was subsequently doped with 3 mol% cesium formate under nitrogen atmosphere, reduced with a 2 vol% H_2/N_2 mixture, and then tested for higher alcohol synthesis under various reaction conditions. Additional testing was carried out, and a manuscript was submitted for presentation at a symposium sponsored by the Division of Fuel Chemistry at the national meeting of the American Chemical Society in Anaheim, CA in May 1995. The manuscript [8] is entitled "Higher Alcohol Synthesis Over a $Cs-Cu/ZnO/Cr_2O_3$ Catalyst: Effect of the Reaction Temperature on Product Distribution and Catalyst Stability."

As described in the manuscript and in the text below, the influence of reaction temperature on methanol and higher alcohol synthesis has been investigated in the range of 310-340°C. Optimal conditions for selective production of 2-methyl primary alcohols included a reaction temperature of 340°C and synthesis gas $H_2/CO = 0.75$. Deactivation features were observed after 300 hr on stream, but no significant growth of Cu° crystals or reduction in surface area was observed for the catalyst after testing.

Introductory Remarks. The $Cu/ZnO/M_2O_3$ systems (M = trivalent metal) are well-known catalysts for methanol and higher alcohol synthesis (HAS) [9-12]; their performances are reported in the literature with particular attention being paid to the optimization of both the catalyst composition (amount of alkaline dopant, metal ion ratios) and the operating conditions [10-13]. The application of these catalysts is commonly limited to reaction temperatures not exceeding 310-325°C in order to avoid sintering phenomena that are recognized as the major constraint and drawback of all the copper-containing catalysts. At these temperatures, methanol formation is highly favored, and only by carrying out the reaction at low H_2/CO ratios can significant quantities of C_{2+} oxygenates be obtained. No specific studies have so far addressed the thermal stability of Cu/ZnO-based systems at high temperatures. However, the strong demand for selective production of branched higher oxygenates supports more extensive exploration of the range of allowable reaction temperatures that can be utilized with copper-based catalysts. Indeed, an increment in the temperature is expected to result in the desired promotion of higher alcohol production and a concurrent decrease in methanol formation. In the following, a study of the effect of reaction temperature on HAS over a Cs-doped $Cu/ZnO/Cr_2O_3$ catalyst is presented, and the principal interests are the changes in the product distribution and the catalyst thermal stability.

Catalyst Preparation. The methodology has been described by Nunan et al. [11,14], and consists of the precipitation of a hydrotalcite-like precursor $Cu_{2.4}Zn_{3.6}Cr_2(OH)_{16}CO_3 \cdot 4H_2O$ [15], followed by stepwise calcination to 350°C to give the mixture of oxides, $CuO/ZnO/Cr_2O_3$. Cesium doping was achieved by adding the catalyst to a N_2-purged aqueous solution of CsOOCH, which was then slowly evaporated to dryness under flowing N_2. The amount of

dopant (3 mol%) was chosen on the basis of previous studies of the optimal catalyst composition with respect to higher alcohol synthesis [11]. The catalyst was finally reduced with a 2 mol% H_2/N_2 mixture at 250°C.

Activity Tests. The apparatus has been extensively described elsewhere [16]. It is noted that charcoal and molecular sieve traps, an internally copper-lined stainless-steel reactor, as well as a copper thermocouple-well were used during the catalytic testing to prevent the formation and deposition of iron-carbonyls, which are well-known deactivating agents [17,18]. The catalysts were tested under steady-state conditions at 7.6 MPa with synthesis gas of various H_2/CO compositions flowing with a gas hourly space velocity of 5300 l/kg cat/hr. The reaction temperature was varied between 310 and 340°C.

The exit product mixture was sampled every 30-60 min using an in-line, automated, heated sampling valve and analyzed in a Hewlett-Packard 5390 gas chromatograph. The products were analyzed *via* a Poraplot-Q capillary column alternatively connected to a flame ionization detector and to a thermal-conductivity detector (TCD) and a Molsieve capillary column connected to TCD. The sensitivity factors of the instrument were determined on the basis of calibrated mixtures. The gas-phase on-line analyses were coupled with the analysis of liquid samples collected downstream from the reactor (atmospheric pressure) by liquid nitrogen cooled traps. The identification of the products (more than 50 components) was obtained by comparison of their retention times with those of known standards and from analysis of the liquid samples by a HP GC/MS instrument. All of the experimental data were obtained in a steady-state regime that was reached about 6-8 hr after setting the operating conditions.

Catalyst Characterization. BET measurements and XRD analyses were performed at each stage of the catalyst preparation and after testing to determine the catalyst surface area and crystalline phases, respectively.

Effect of the Reaction Temperature on the Product Distribution. In Figure 3.3.1, the productivities of the most abundant oxygenated products are reported as a function of the reaction temperature, which was increased from 310°C up to 340°C over a period of about 160 hr. As the temperature was increased, a decrease of methanol productivity was observed, in line with the thermodynamic constraints that govern methanol synthesis. As shown in Figure 3.3.1a, the productivities of all the linear higher alcohols exhibited decreasing trends with increasing reaction temperature. In fact, the product mixture tends to become depleted in intermediate species (ethanol, propanol) and more enriched in the branched oxygenates that play a terminal role in the chain-growth process. At 325°C, a promotion of all the 2-methyl alcohols was observed (Figure 3.3.1b). It is noted that the molar ratio between methanol and the totality of α-branched alcohols passed from a value of about 16 at 310°C to the value of about 5 at 340°C. In the case of secondary alcohols (whose productivities are summed in Figure 3.3.1c with those of the corresponding ketones), it is observed that high temperatures favor the formation of high molecular weight species (e.g., 2-methyl-3-pentanol) at the expense of the intermediate species (e.g., 2-butanol).

Figure 3.3.1 - Experimental Effect of Reaction Temperature on Methanol and Higher Oxygenates Productivities

In 1-c: 2met-3Pent = 2methyl-3-pentanol + 2 methyl-3-pentanone, 3-Pent. = 3-pentanol + 3-pentanone, 3met-2But. = 3-methyl-2-butanol + 3-methyl-2-butanone, 2-But. = 2 butanol + 2-butanone.

Operating Conditions: $H_2/CO = 0.45$, P = 7.6 MPa, GHSV = 5300 l/kg cat/hr.

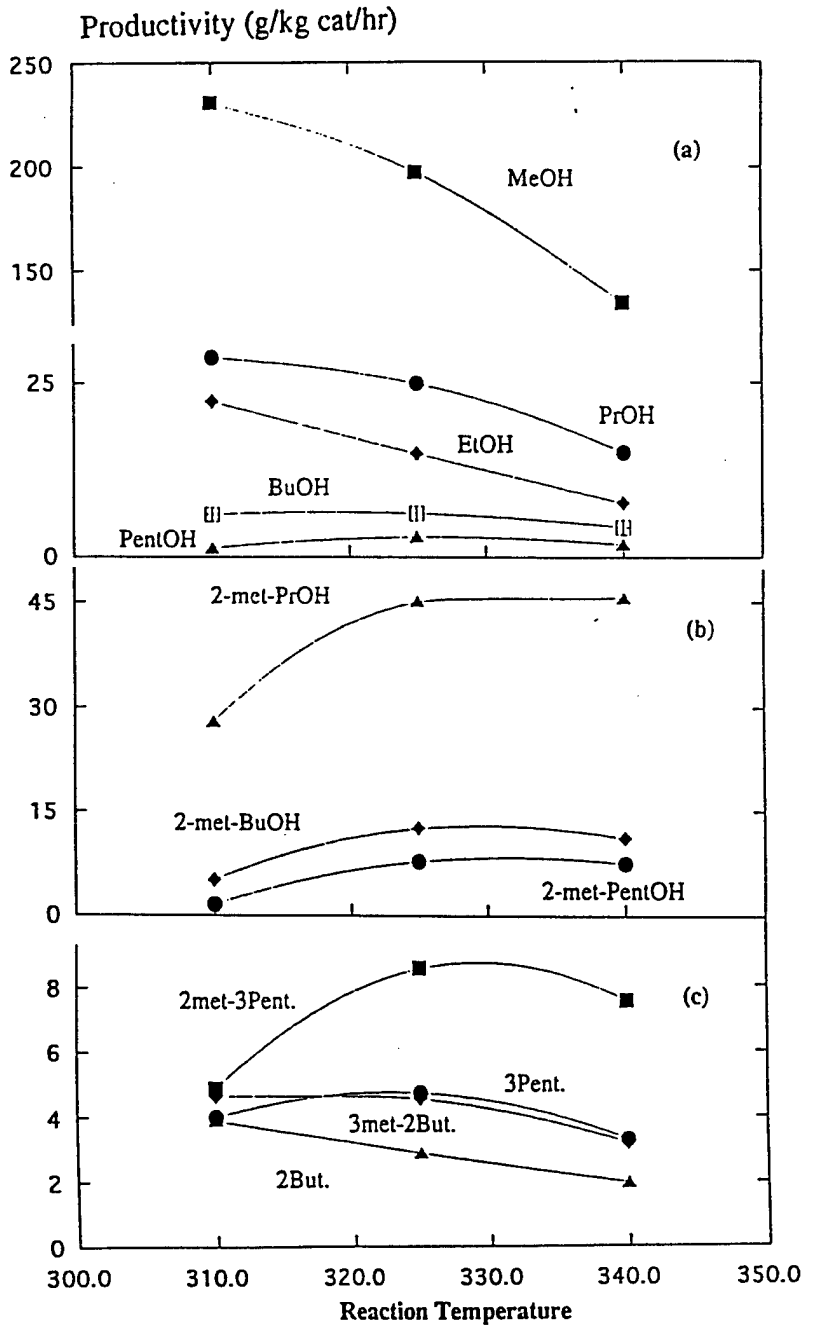

The formation of methane and C_2^+ hydrocarbons was also observed to increase with increasing reaction temperature (Figure 3.3.2). The overall production of hydrocarbons, equal to 15.7 g/kg cat/hr at 310°C, grew to the value of 39.4 g/kg cat/hr at 340°C. It is worth noting that, contrary to the case of oxygenates, hydrocarbons appear to keep an almost constant relative product distribution, which could support the hypothesis of a formation pattern independent from the higher alcohol chain-growth process.

Finally, it is noted that the productivities of all the methyl-esters detected in the product mixture decreased monotonically with increasing reaction temperature. This trend was especially evident in the case of methyl-formate and methyl-acetate, while it was less pronounced for the higher homologs (methyl-propionate, methyl-isobutyrate, methyl-butyrate).

High Reaction Temperature: Effect of H2/CO Ratio. At the reaction temperature of 340°C, kinetic runs were performed to investigate the combined effects of high temperature and H_2/CO feed ratio on HAS product distribution. The results are reported in Figure 3.3.3, and the data show that an excess of H_2 exclusively promoted methanol formation. The production of higher oxygenates appears to be significantly inhibited at high H_2/CO ratios. Specifically, all of the primary alcohols tended to show a maximum in productivity, with the highest value being associated with the H_2/CO value of 0.75 (Figure 3.3.3a,b).

With respect to the formation of hydrocarbons, the data reported in Figure 3.3.4 indicate that while the synthesis of C_2^+ hydrocarbons was strongly slowed by decreasing CO partial pressure, methane productivity was approximately constant as a function of the H_2/CO ratio.

High Reaction Temperature: Catalyst Stability. The operating conditions of T = 340°C, H_2/CO = 0.45, 7.6 MPa, and GHSV = 5300 l/kg cat/hr were periodically reproduced in order to check the stability of the catalyst. The results of the experiments are reported in Figure 3.3.5, where the averaged FID signals, in arbitrary units, for the most abundant products have been plotted *vs* the time of testing. As previously noted, a period of about 160 hr occurred before the final temperature of 340°C was reached, and at this high temperature a stable catalytic activity was observed during 125 hr. Subsequently, a slow loss of selectivity of the higher oxygenates in favor of an increment in methanol productivity was detected. Similar results were obtained in the past when deactivation caused by the deposition of iron carbonyls onto Cu/ZnO catalysts was studied [17]. Even though the cause of the behavior shown in Figure 3.3.5 cannot be assessed, Cu° sintering can be excluded as playing a major role, where the XRD pattern of the tested catalyst (300 hr on stream at 340°C) revealed the presence of metallic copper with crystallite size in the range of 100A, which is comparable with the dimension of Cu° crystallites observed in in the binary Cu/ZnO systems after the reduction stage and before testing [17]. Moreover, BET measures showed that no reduction in the catalyst surface area occurred during the kinetic runs, being 85 m2/g and 89 m2/g before and after testing, respectively.

Figure 3.3.2 - Effect of Temperature on C_1-C_6 Hydrocarbon Production and Distribution

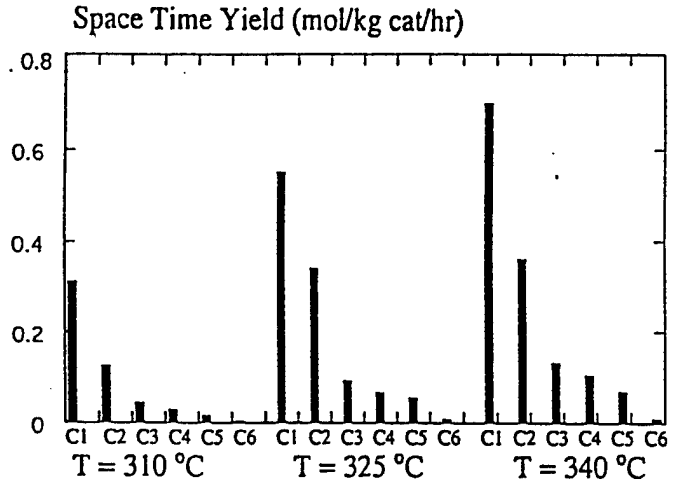

Figure 3.3.3 - Effect of H_2/CO Ratio; T = 340°C, P = 7.6 MPa, GHSV = 5300 l/kg cat/hr

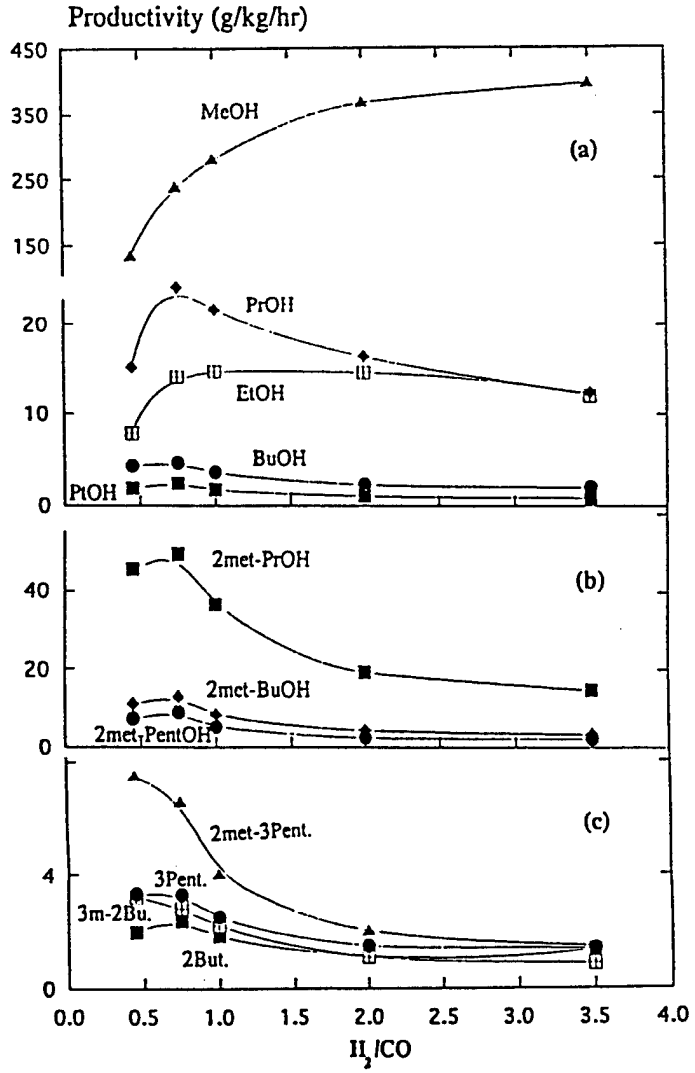

Figure 3.3.4 - Effect of H_2/CO Ratio Hydrocarbon Formation. Conditions as in Figure 3.3.3

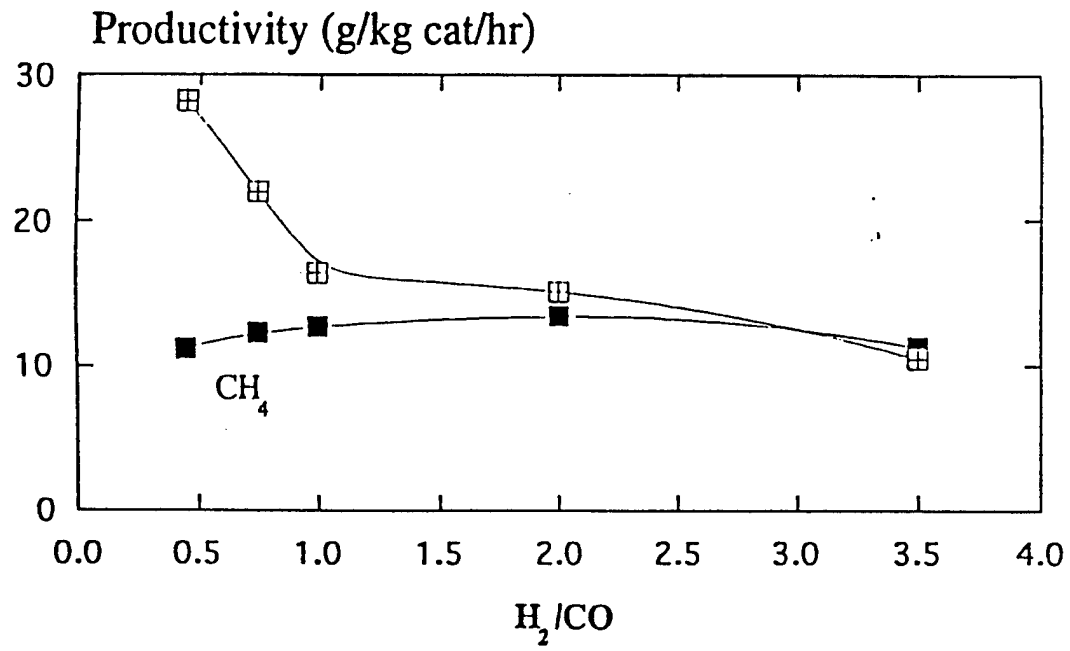

Figure 3.3.5 - Change of Product Distribution with Time as Detected by FID

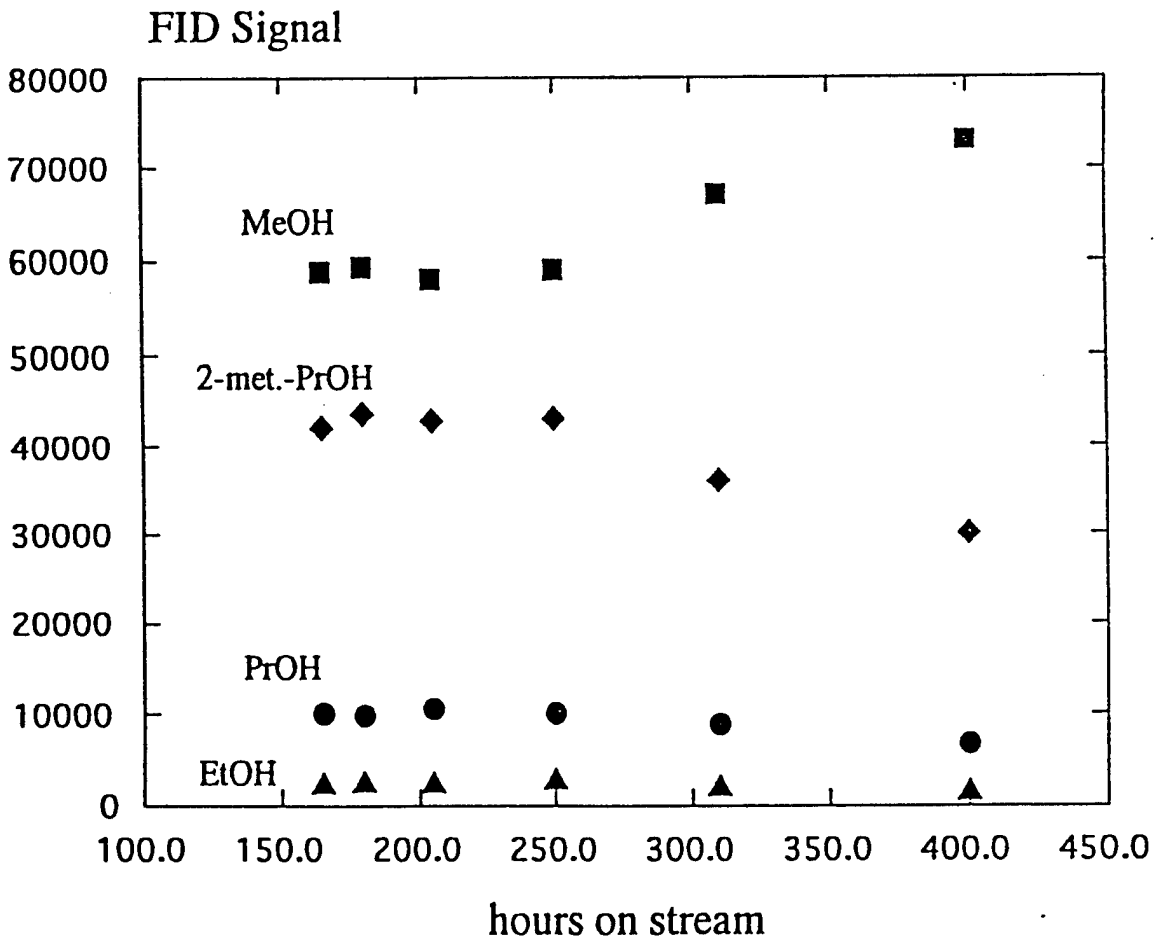

Conclusions. The experimental results for the synthesis of higher alcohols over the $Cs/Cu/ZnO/Cr_2O_3$ catalyst suggest that:

(1) The productivity of α-branched species benefits significantly from an increment of the reaction temperature to 325°C. For further increments of temperature, the productivities of higher alcohols are almost constant, but the methanol/higher alcohols molar ratio increases progressively.

(2) At high temperature, the H_2/CO feed ratio of 0.75 is optimal with respect to higher oxygenate formation. Under such conditions, an equal amount of methanol but *twice* the amount of branched higher alcohols can be obtained, compared to the optimal low temperature conditions (T = 310°C, H_2/CO = 0.45).

(3) No significant Cu sintering or surface area reduction occurred upon testing at the reaction temperature of 340°C; however, iron-carbonyl formation and deactivation of the catalysts under high temperature conditions need to be studied further.

REFERENCES

1. Lietti, L., Sun, Q., Herman, R. G., and Klier, K., "Kinetic Evaluation of the Direct Synthesis of Ethers From Alcohols Over Sulfonated Resin Catalysts," to be presented at the *First World Conference on Environmental Catalysis* (Pisa, Italy) and to be published in Catal. Today, 8 pp (1995); accepted based on a 2-page abstract.

2. Klier, K., Herman, R. G., Lietti, L., Sun, Q., Johansson, M. A., and Feeley, O. C., Quarterly Technical Progress Report on "Oxygenates *via* Synthesis Gas" for January-March 1994.

3. Klier, K., Herman, R. G., Sun, Q., Johansson, M. A., Lietti, L., and Feeley, O. C., Quarterly Technical Progress Report on "Oxygenates *via* Synthesis Gas" for April-June 1994.

4. Sun, Q., Lietti, L., Herman, R. G., and Klier, K. "Mechanistic Studies of the Pathways Leading to Ethers *via* Coupling of Alcohols," Preprint, Div. Fuel Chem., ACS, 40 (1995); in press.

5. Nordberg, R., Albridge, R. G., Bergmark, T., Ericsson, U., Hedman, J., Nordling, C., Siegbahn, K., and Lindberg, B. J., Arkiv för Kemi, 28, 257 (1968).

6. Marsili, M. and Gasteiger , J., Croat. Chem. Acta, 53, 601 (1980).

7. Nunan, J. G., Himelfarb, P. B., Herman, R. G., Klier, K., Bogdan, C. E., and Simmons, G. W., Inorg. Chem., 28, 3868 (1989).

8. Beretta, A., Sun, Q., Herman, R. G., and Klier, K., "Higher Alcohol Synthesis Over Cs-Doped Cu/Zn/Cr Oxide Catalysts: Effect of Reaction Temperature on the Product Distribution and Catalyst Stability," Preprint, Div. Fuel Chem., ACS, 40 (1995); in press.

9. Natta, G., Colombo, U., and Pasquon, in *"Catalysis,"* Vol. 5, Chap. 3, ed. by P. H. Emmett, Reinhold (1957).

10. Smith, K. J. and Anderson, R. B., J. Catal., 85, 428 (1984).

11. Nunan, J. G., Herman, R. G., and Klier, K., J. Catal., **116**, 222 (1989).

12. Herman, R. G., in *"New Trends in CO Activation,"* ed. by L. Guczi, Elsevier, Amsterdam, 265 (1991).

13. Boz, I., Sahibzada, M., and Metcalfe, I., Ind. Eng. Chem. Res., 33, 2021 (1994).

14. Nunan, J. G., Himelfarb, P. B., Herman, R. G., Klier, K., Bogdan, C. E., and Simmons, G. W., Inorg. Chem., 28, 3868 (1989).

15. Busetto, C., Del Piero, G., Manara, G., Trifiro, F., and Vaccari, A., J. Catal., 85, 260 (1984).

16. Nunan, J. G., Bogdan, C. E., Klier, K., Smith, K. J., Young, C.-W., and Herman, R. G., J. Catal., **116**, 195 (1989).

17. Bogdan, C. E., Nunan, J. G., Santiesteban, J. G., Herman, R. G., and Klier, K., in *"Catalysis-1987,"* ed. by J. W. Ward, Elsevier, Amsterdam, 745 (1988).

18. Hindermann, J. P., Hutchings, G. J., and Kiennemann, A., Catal. Rev.-Sci. Eng., 35, 1 (1993).

II. 2QFY95 Objectives

Future plans for Task 3.3 will focus on the following area:

3.3 New and improved catalysts and processes for the synthesis of mixed higher alcohol and other oxygenates.

3.3.2 The Effect on Performance of Axial Temperature Gradients in the Packed Bed

3.3.2.1 Motivation for Investigation

Thus far, all modifications to the preparation procedure for Falter's Li/Mn/Zn/Zr catalyst have resulted in approximately the same performance in syngas or syngas-plus-methanol conversion. Therefore, the possibility exists that catalyst preparation may not be the key issue in trying to reproduce Falter's results. Thus, differences in testing methods between Air Products and Falter's

original work have been considered to account for the discrepancy between the performance results obtained in this work and his.

One difference noted was that the design of Falter's packed bed reactor was quite different from the design of either packed bed Reactor #1 or Reactor #2. Falter's reactor, which was very long and narrow, resulted in a very large axial temperature gradient (temperature increased steeply with axial distance down the bed). By contrast, the design of Reactors #1 and #2 attempted to minimize axial gradients (i.e., approximate isothermality) by using a relatively short reactor bed located deep within a heated zone surrounded by an aluminum block to provide good thermal conductivity. The steep temperature gradient observed in Falter's work, caused by the exothermicity of the syngas reaction coupled with reactor geometry, may have impacted the measured performance of the Li/Mn/Zn/Zr-based catalyst in Falter's work.

One hypothesis is that the steep gradient could have provided a unique, but favorable, set of conditions for the production of isobutanol. In fact, the existence of a cool upstream reaction zone followed by a hotter downstream reaction zone is the concept that the current work is attempting to demonstrate in the two-stage isobutanol synthesis process (low temperature methanol synthesis followed by methanol conversion to isobutanol). To investigate the influence of axial temperature gradients in more detail, Reactor 3 was constructed to approximate Falter's original reactor design, in an attempt to create the same steep axial temperature gradient during reaction. It was deliberately designed long and narrow without an aluminum heating block to allow for axial temperature gradients.

3.3.2.2 Results Obtained Using Reactor #3

Since the catalyst bed was much longer in this reactor than in Reactors #1 and #2, more catalyst was required to fill it (20 g vs. 5 g previously used); thus it was necessary to precipitate more Li/Mn/Zn/Zr catalyst. Since Pd impregnation was previously shown to have no impact on performance, the Li/Mn/Zn/Zr material, without impregnated Pd, was tested in this new reactor. This new sample of catalyst was prepared in the 3 liter precipitator without N_2 purge at pH=10, and was tested at the previously used conditions of 1500 psig and a GHSV of 10,000 std.lit./kg-hr of 50% H_2/50% CO feed gas.

The measured axial temperature gradient during this run is compared with Falter's gradient in Figure 3.3.6. Clearly, the new reactor design was successful in establishing a steep temperature gradient comparable to Falter's, though Falter's is slightly steeper in the first half of the bed.

Figure 3.3.6 - Packed-Bed Axial Temperature Gradients during Syngas Conversion
Catalyst: Li/Mn/Zn/Zr (#14183-18-1)
No Catalyst in Microclave
Run: 14047-25 1500 psig, 425°C, GHSV=10000 std.lit./kg-hr Syngas Comp.: 50%H_2/50%CO
Packed Bed Reactor #3

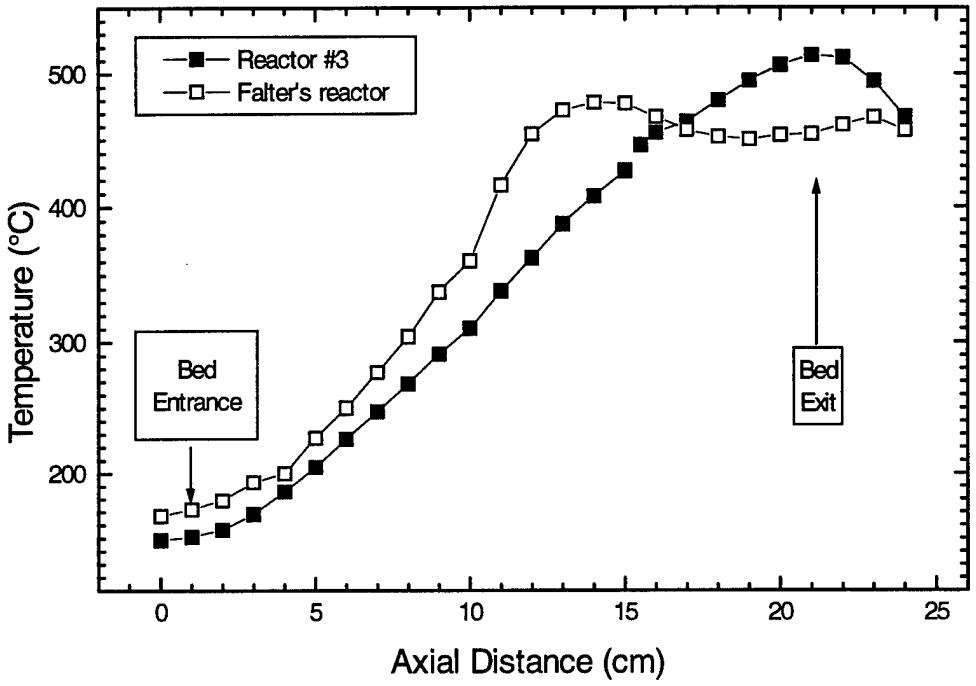

Even though a steep axial temperature gradient was established in these tests, this resulted in a lower measured catalyst performance than that observed using the old reactor. Table 3.3.1 shows the performance results for syngas conversion and methanol-plus-syngas conversion for the Li/Mn/Zn/Zr catalyst, and syngas conversion for the Pd-impregnated version of this catalyst. Compared with the previously discussed results obtained using Reactors #1 and #2, the isobutanol production rate is much lower in Reactor #3, and lower than expected based on Falter's data.

Evidently, the existence of a steep axial temperature gradient in the reactor does not explain the high performance measured in Falter's original work. The reason that Falter's original performance cannot be reproduced is still not known. However, the current results indicate that it is the catalyst itself rather than the method of testing. Further investigation may reveal the reason.

Table 3.3.1 - Effect of Imposed Axial Temperature Gradient on Performance
Catalysts: Li/Mn/Zn/Zr (#14183-18-1) and Pd/Li/Mn/Zn/Zr (#14183-18-2)
No Catalyst in Microclave
Runs: 14047-25, -34 1500 psig, 425°C, GHSV=10000 std.lit./kg-hr,
Syngas Comp.: 50%H_2/50%CO
Packed Bed Reactor #3

		Reactor Exit Rate (g/kg-hr)				
catalyst	reactor feed	methanol	ethanol	1-propanol	isobutanol	DME
Li/Mn/Zn/Zr	syngas	30.8	0.3	9.3	20.4	22.7
Li/Mn/Zn/Zr	syngas + 10 mole% methanol	36.5	0.3	8.8	22.0	132
Pd/Li/Mn/Zn/Zr	syngas	39.9	0.3	10.0	31.5	34.5

3.3.2.3 Catalyst Analysis

Elemental Analysis and BET Surface Area of Catalysts used in Reactor #3
Table 3.3.2 shows the results of elemental analysis and BET surface area determinations for unused samples of the catalysts used in packed bed Reactor #3. Also shown are results reported in Falter's thesis for his version of the catalyst. The catalysts used in the current work are significantly lower in Li content than Falter's version. However, results reported previously indicate that Li content had no impact on performance. For unknown reasons, the Zn content of these catalysts was much higher than that reported by Falter. The proportions of the starting materials for the catalysts were the same as Falter used in his preparation. Measured BET surface area for the Pd-impregnated version was comparable to that for Falter's catalyst.

Table 3.3.2. Elemental Analysis and BET Surface Area of Li/Mn/Zr/Zn and Pd/Li/Mn/Zr/Zn Catalyst Used in Reactor #3

Element	Analysis (wt%)		
	Li/Mn/Zn/Zr (#14183-18-1)	Pd/Li/Mn/Zn/Zr (#14183-18-2)	Falter's Pd/Li/Mn/Zn/Zr Catalyst
manganese (Mn)	13.8	14.3	15.4
zirconium (Zr)	35.3	36.0	30.5
zinc (Zn)	16.0	16.9	8.6
lithium (Li)	0.24	0.23	1.5
palladium (Pd)	---	0.22	Not reported
BET Surface Area (m2/g)	246	193	209

The elemental analysis and surface area measurements provide no significant clues as to why Falter's performance cannot be reproduced.

Thermogravimetric Analysis (TGA) of Fresh and Used Catalysts

The effect of temperature on the structure and composition of the Li/Mn/Zn/Zr-based catalyst was investigated in light of the steep temperature gradients observed in Falter's work. To investigate possible thermally induced changes in the catalyst in more detail, fresh and used samples of a Li/Mn/Zn/Zr material (#14183-11-1) were examined by TGA. This catalyst was used in run 14047-4 (performance results were previously presented in Table 3.3.1). Nitrogen, air, and H_2 were used for both the fresh and used materials to compare the effect of inert, oxidizing, and reducing atmospheres, respectively. For these investigations, a new sample was loaded in the TGA for each run, i.e., the individual TGA samples were not reused.

Figures 3.3.7 and 3.3.8 show TGA results for the three gases for the fresh and spent Li/Mn/Zn/Zr samples, respectively. For the fresh catalyst, the weight loss curves for air and N_2 are very similar. There is an initial large weight loss before 100°C that is most likely due to H_2O adsorbed from the atmosphere during handling. However, for H_2 on the fresh catalyst there are two distinct weight losses at higher temperatures: between approximately 300°C and 400°C and between 500°C and 800°C. The weight loss from 500°C to 800°C also occurs for H_2 TGA in the used sample (Figure 3.3.8), but the lower temperature loss (300°C to 400°C) is absent. Also evident in the TGA results for the used sample is a considerable weight gain in air between 300°C and 800°C.

The TGA results are interpreted as follows, considering that the fresh catalyst most likely consists of the metal oxides, Li_2O, MnO, ZnO, and ZrO_2. The 20% weight loss between 500°C and 800°C for H_2 TGA, which occurs for both fresh and spent samples, is likely due to the vaporization of metallic, elemental zinc, which had been previously produced by reduction of ZnO (ZnO is the most easily reduced oxide present). The magnitude of the weight loss is consistent with the total quantity of zinc in the catalyst (approximately 24 wt%). Moreover, the temperature range at which the weight loss occurs is consistent with the volatility of elemental zinc (Zn melts at 520°C, boils at 911°C, and has a significantly large vapor pressure between 500°C and 800°C). The vaporization of Zn has been confirmed by elemental analysis of the spent sample after the H_2 TGA, which showed no Zn present.

The cause of the lower temperature (300° to 400°C) weight loss for the fresh sample during H_2 TGA is not known, but probably represents reduction of some part of the catalyst. Since this weight loss does not occur in the used sample, the unknown reduction has probably already occurred during exposure of this sample to syngas at the 425°C reaction temperature. The weight gain during the air run on the used sample probably indicates a reoxidation of this reduced material. This weight loss probably does not correspond to reduction of ZnO to Zn, since Zn vaporization would be expected but does not occur in N_2 for the used sample. Further analysis is necessary to identify the cause of the 300-400°C weight loss in H_2 for the fresh sample.

The TGA results provide no clues as to why we have not been able to reproduce Falter's catalyst performance. The most dramatic, thermally-induced change in the catalyst is the apparent loss of Zn at temperatures greater than 500°C. Our reaction temperature (425°C in run 14047-4) and Falter's peak reactor temperature (approximately 475°C) are less than the temperature range at which reduction of ZnO and vaporization of Zn take place. Apparently, no major thermally-induced changes in the catalyst occur at temperatures near the reaction temperature range of interest (425°C-475°C); at least none that can be identified by TGA.

3.3.7 - TGA of Fresh Li/Mn/Zn/Zr Catalyst

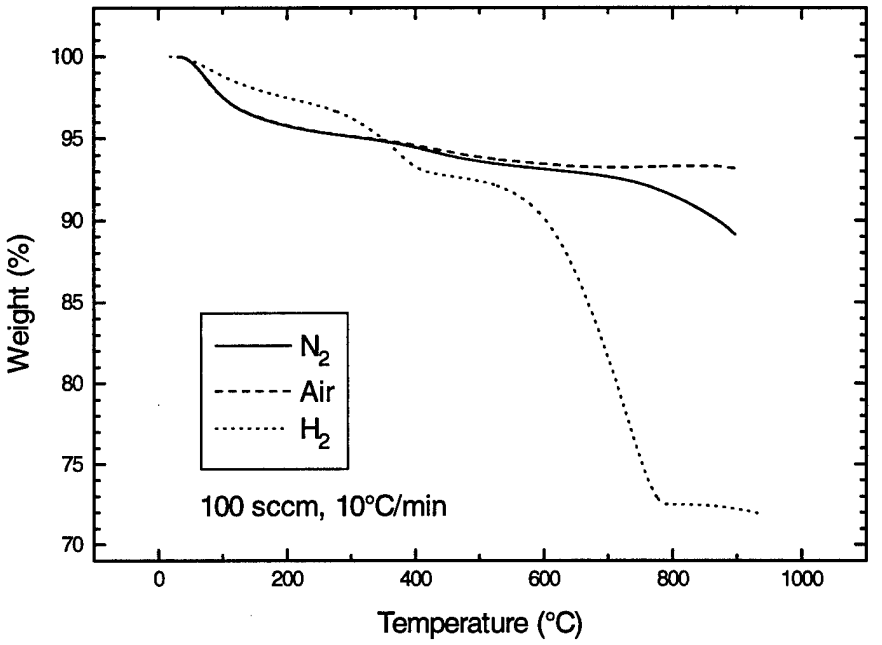

Figure 3.3.8 TGA of Li/Mn/Zn/Zr Used in Syngas Reaction

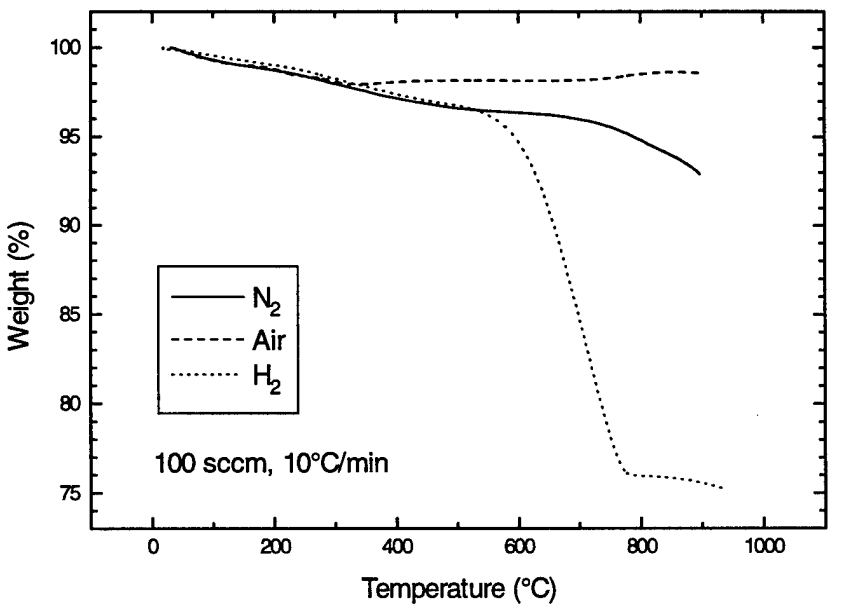

3.3.2.3 Effect of Precipitating with Potassium Hydroxide instead of Lithium Hydroxide

Thus far, the investigations indicate that the performance of the Li/Mn/Zn/Zr-based catalyst is fairly insensitive to preparation procedure, metal precursors, and whether or not Pd is present. To provide more information on the influence of preparation procedure, the effect of the alkali metal used in the preparation was investigated. To this end, the precipitation was done with KOH instead of the previously used LiOH. Falter had also prepared catalysts with both Li and K, and found Li to be the most effective at promoting isobutanol synthesis. This catalyst was prepared at pH=10 without N_2 purge.

Results for the performance of Pd/K/Mn/Zn/Zr for syngas conversion and syngas-plus-methanol conversion are shown in Table 3.3.3. Comparison with the previously reported results for the lithium-precipitated catalysts indicate that the Li-containing catalyst is slightly more effective at producing isobutanol than the K-containing catalyst for both types of feed. This trend is in agreement with the previous results of Falter. The K-containing catalyst is not effective at methanol-plus-syngas conversion to isobutanol either. In addition, the K-containing catalyst exhibited a higher rate and selectivity to hydrocarbons.

Table 3.3.3 - Performance Results for Pd/K/Mn/Zn/Zr

Catalyst: Pd/K/Mn/Zn/Zr (#14183-14-2)
No Catalyst in Microclave
Run: 14047-10 1500 psig, 425°C, Syngas Comp.: 50%H_2/50%CO
Packed Bed Reactor #2 (Copper-Lined)

		Production Rate at Packed Bed Exit (g/kg-hr)*					
Feed Gas	Syngas GHSV (std.lit./ kg-hr)	Methanol	Ethanol	1-propanol	Isobutanol	C_1-C_6 Hydro-carbons	DME
syngas	10000	113	0.3	8.3	45.0	47.2	4.9
syngas	15000	162	0.5	11.0	59.7	53.6	6.2
syngas + methanol*	15000	233	0.5	10.1	59.8	44.0	100

*methanol feed concentration=14 mol% (addition rate=3400 g/kg-hr).

3.3.2.4 Summary of Status on Two Bed Work

The development of a two-stage process for the production of isobutanol remains a challenge. Though Falter's original work indicates that a Pd/Li/Mn/Zn/Zr catalyst would be very effective as the second-stage catalyst in this process, that effectiveness could not be reproduced in the present work.

Table 3.3.4 shows the extent to which the results are disparate. Falter's reaction conditions were not reproduced exactly in the present work, but the conditions are comparable. Shown in Table 3.3.4 are results from Falter's thesis compared with results obtained in the present work, for syngas conversion and syngas-plus-methanol conversion. For syngas conversion, isobutanol productivity observed in this work is about 50% of that seen by Falter. However, the larger

difference is in syngas-plus-methanol conversion, where Falter's isobutanol rate is 4.5 times that measured in this work under comparable reaction conditions.

The performance of the Li/Mn/Zn/Zr-based catalysts prepared in the present work, particularly with respect to syngas-plus-methanol conversion to isobutanol, is relatively insensitive to catalyst preparation variables such as the:

(1) presence or absence of supported Pd
(2) Li content
(3) extent of mixing during precipitation
(4) drying and pelletizing procedure
(5) inclusion or exclusion of N_2 purging during precipitation.

In addition, the performance of the Li/Mn/Zn/Zr-based catalysts prepared in this work have been shown to be fairly insensitive to certain variable involved in testing the catalysts, such as the:

(1) reactor material of construction
(2) presence or absence of steep axial temperature gradients.

The reason why Falter's original work can not be reproduced is, at this time, a mystery. The problem is, most likely, the inability to reproduce the exact catalyst. Work at Aachen has reproduction of this catalyst as a primary goal. No further work will be done on the two bed process until the original preparation has been reproduced at Aachen. Solving this mystery will be especially difficult given the absence of a sample of Falter's original material and the scarcity of characterization work done on the sample. However, the remarkable ability of that material to catalyze syngas-plus-methanol conversion cannot be ignored if economical isobutanol production is to continue to be a development target.

Table 3.3.4 - Comparison of Performance Results from This Work with Results Published by Falter

Catalyst	Temp. (°C)	Press. (psig)	Feed Gas	Syngas GHSV (hr^{-1})	Production Rate (g/liter-hr) methanol	Production Rate (g/liter-hr) isobutanol
Falter - Pd/Li/Mn/Zn/Zr*	427	1435	50% H_2/50% CO	20,000	45	165
This work - Pd/Li/Mn/Zn/Zr**	425	1500	50% H_2/50% CO	19,500	188	84
Falter - Pd/Li/Mn/Zn/Zr*	427	1435	43% H_2/43% CO/14% methanol	15,000	85	450
This work - Pd/Li/Mn/Zn/Zr**	425	1500	43% H_2/43% CO/14% methanol	19,500	323	101

* W. Falter, PhD thesis, RWTH-Aachen, 1988, pp. 161.
** This work, run 14047-7.

3.3.2.5 Isobutanol Synthesis in a Three Phase System

Engineering Aspects

The activities within the last quarter of the year were testing catalysts and improving our analytical procedures. The unit is now equipped with two high-grade analysis systems. The best results found in catalytic runs showed a selectivity to isobutanol in the liquid product of more than 25% with a space-time yield over 300 g/(l*h).

1. Slurry Reactor

The slurry reactor has nearly been finished. A reamer needed for machining the inner surface of the reactor was four weeks late. First tests with this continuous slurry reactor will be in February 1995.

2. Fixed Bed Reactor

To study the impact of temperature in more detail, the temperature indicating and controlling system at the fixed bed reactor was optimized. Initially the process variables to control the jacket heatings were obtained directly at the jacket heatings themselves according to Falter. The temperature profile was determined by a combination of external heating, the strongly exothermic reaction and the loss of heat. Under reaction conditions, the three thermocouples inside the fixed bed always indicated a higher temperature than the temperature at the jacket heatings.

These three thermocouples show that process temperature controls jacket heating. Thus, the temperature inside the fixed bed can be controlled exactly; temperature gradients must be produced artificially.

3. On-Line Screening

The unit has been equipped with a capillary system for the calibration gas. With this calibration gas a random failure was found. The on-line screening system consisting of bypass, sample injector, gas chromatograph and integrator was checked and optimized. Some experimental difficulties due to instrumental failure were found and fixed. Residual high boiling products remaining in the bypass capillary were found to vary the pressure drop along the bypass. To avoid the influence of this effect on the reliability of the analysis, the possibility of injecting the sample without pressure will be investigated in January.

4. Product Sampler

The product sampler as described in a previous progress report has been finished and is operating well. It was tested in several runs using a downstream trap cooled by dry ice or liquid nitrogen. The product sampler operates with a mass loss of 30% (depending slightly on the gas mass stream). The composition of probes collected in the product sampler and in the topped trap were identical, i.e., the product composition was not effected.

5. Experiments

Irrespective of the results shown at the beginning, the influence of variations in reaction conditions on isobutanol synthesis are discussed in below in terms of:

- The effect of a temperature gradient at the entrance zone of the fixed bed inside the reactor and
- Changes in reduction conditions and the use of glass particles for the fixed bed within this quarter.

As a result of changing temperature measurement, the axial temperature gradient must be produced artificially. Switching off heating jacket 2W1 decreases the temperature TIC 205 by about 90°C. The resulting temperature gradient is 1.5°C/mm. The effect of this gradient compared with a gradient-free run is non-uniform and depends on pressure, gas mass flow and to a lesser extent on the catalyst. The effect on the space-time yield of methane and methanol was found to depend on the residence time given by pressure and gas mass flow. A long residence time at the heated entrance zone filled only with glass particles led to an increased methane production. It was observed that the amount of formed methane in these cases was up to 2.5 times higher than in the case where the first heating jacket was switched off. In contrast methanol production showed the opposite behavior, having maximum productivities when the first heating jacket was switched off. However, the space-time yield i-BuOH remained nearly constant.

After reduction conditions were changed and glass particles were used for the fixed bed, catalyst BJ 17 was tested a second time and showed a different behavior. The selectivity to isobutanol decreased, and its space-time yield increased. The results of the older run CH 14 and the actual run CH 28 are listed in Table 3.3.5.

Table 3.3.5 - Results from Catalyst Tests in a Fixed Bed Reactor

org. information test No.: cat. No.:	CH 14:02 BJ 17	CH 14:03	CH 28:02	CH 28:03
set point				
GHSV [1/h]	20000			
pressure [bar]	236	236	250	250
temperature [°C]	375	400	445	415
volume flow [Nl/h]	100	100	80	80
results				
% Methanol	18.52	9.72	31.95	62.18
% 2,4-Dimethylpentanon-3	0.98	1.05	1.37	0.66
% n-Propanol	1.22	0.96	0.80	0.60
% i-Butanol	49.16	46.60	27.36	16.28
% 2,4-Dimethylpentanol-3	2.11	1.41	0.69	0.35
% 2-Methylbutanol-1	6.01	5.19	3.33	1.53
% 2-Methylpentanol-1	2.62	3.60	2.60	1.01
space-time yield i-BuOH [g/(l*h)]	45	62	311	142

The catalyst is from the same batch. The differences in the reaction conditions are minor. Higher set temperatures in run CH 28 are the result of changing the indicating temperature and controlling system. In run CH 14 the set temperature was measured at the jacket heatings. The fixed bed temperature was about 20°C higher. In run CH 28 the set temperature was measured at the fixed bed.

In contrast to the explanation in his thesis, Falter reduced the catalysts both inside and outside the reactor in a special apparatus. The differences in both reduction methods are substantial. We have tested both methods. The reaction conditions of each run are listed below:

Scheme 1: Reduction Conditions for Run CH 14

gas:	hydrogen
mass flow:	60 Nl/h
pressure:	ambient pressure
heating rate:	< 4 °C/min
temperature:	200°C
reduction time:	2h

Scheme 2: Reduction Conditions for Run CH 28

gas:	hydrogen
mass flow:	30 Nl/h
pressure:	3 MPa
heating rate:	4 °C/min
temperature:	225°C
reduction time:	2h

The second significant modification is the the use of glass particles in the fixed bed since the inner tube was changed. Glass particles were also used by Falter.

As a result of these experiments, another batch of catalyst BJ 17 will be prepared according to the formerly used procedure and tested in further runs. Both reduction methods will be used to obtain more information. The influence of the kind of glass and/or the structure of the fixed bed will be examined, and the set of twelve catalysts will be further tested.

Chemical Aspects

This section will discuss the catalyst design strategy used to optimize the isobutanol catalyst.

1. Coprecipitated Zr/Zn/Mn-Catalysts

The set of Falter catalysts described previously has been completed. A typical procedure for the synthesis of these catalysts is described below:

A solution of $ZrO(NO_3)_2$, $Zn(NO_3)_2$, $Mn(NO_3)_2$ (0.17 mole each) in 1 liter of deionized water was simultaneously added with a 2 M aqueous solution of LiOH (or KOH) into a vessel